


Inhibition of Glucose-6-Phosphate Dehydrogenase Activity Attenuates Right Ventricle Pressure and Hypertrophy Elicited by VEGFR Inhibitor + Hypoxia

Atsushi Kitagawa, Christina Jacob, Allan Jordan, Ian Waddell, Ivan F. McMurtry, and  Sachin A. Gupte

Department of Pharmacology, New York Medical College, Valhalla, New York (A.K., C.J., S.A.G.); Drug Discovery Unit, Cancer Research UK Manchester Institute, University of Manchester, Macclesfield, United Kingdom (A.J., I.W.); and Departments of Pharmacology and Internal Medicine and Center for Lung Biology, College of Medicine, University of South Alabama, Mobile, Alabama (I.F.M.)

Received June 12, 2020; accepted February 16, 2021

ABSTRACT

Pulmonary hypertension (PH) is a disease of hyperplasia of pulmonary vascular cells. The pentose phosphate pathway (PPP)—a fundamental glucose metabolism pathway—is vital for cell growth. Because treatment of PH is inadequate, our goal was to determine whether inhibition of glucose-6-phosphate dehydrogenase (G6PD), the rate-limiting enzyme of the PPP, prevents maladaptive gene expression that promotes smooth muscle cell (SMC) growth, reduces pulmonary artery remodeling, and normalizes hemodynamics in experimental models of PH. PH was induced in mice by exposure to 10% oxygen (Hx) or weekly injection of vascular endothelial growth factor receptor blocker [Sugen5416 (SU); 20 mg kg⁻¹] during exposure to hypoxia (Hx + SU). A novel G6PD inhibitor (*N*-[(3 β ,5 α)-17-oxoandrostan-3-yl] sulfamide; 1.5 mg kg⁻¹) was injected daily during exposure to Hx. We measured right ventricle (RV) pressure and left ventricle pressure-volume relationships and gene expression in lungs of normoxic, Hx, and Hx + SU and G6PD inhibitor-treated mice. RV systolic and end-diastolic pressures were higher in Hx and Hx + SU than normoxic control mice. Hx and Hx + SU decreased

expression of epigenetic modifiers (writers and erasers), increased hypomethylation of the DNA, and induced aberrant gene expression in lungs. G6PD inhibition decreased maladaptive expression of genes and SMC growth, reduced pulmonary vascular remodeling, and decreased right ventricle pressures compared with untreated PH groups. Pharmacologic inhibition of G6PD activity, by normalizing activity of epigenetic modifiers and DNA methylation, efficaciously reduces RV pressure overload in Hx and Hx + SU mice and preclinical models of PH and appears to be a safe pharmacotherapeutic strategy.

SIGNIFICANCE STATEMENT

The results of this study demonstrated that inhibition of a metabolic enzyme efficaciously reduces pulmonary hypertension. For the first time, this study shows that a novel inhibitor of glucose-6-phosphate dehydrogenase, the rate-limiting enzyme in the fundamental pentose phosphate pathway, modulates DNA methylation and alleviates pulmonary artery remodeling and dilates pulmonary artery to reduce pulmonary hypertension.

Introduction

Pulmonary hypertension (PH) is a multifactorial disease that is defined as sustained elevation of pulmonary arterial pressure (Farber and Loscalzo, 2004). The elevation of pulmonary arterial pressure increases right ventricular (RV) afterload, leading to heart failure and death (Runo

and Loyd, 2003). The main vascular changes in PH are vasoconstriction, vascular cell proliferation, and thrombosis. Based on these findings, current standard of care is treatment with vasodilators. However, vasodilators such as endothelin receptor blockers, nitric oxide/nitrates, prostacyclin, and phosphodiesterase-5 inhibitors fail to reverse vascular remodeling, and the long-term prognosis remains poor (Lajoie et al., 2016).

Based on WHO classification, PH is divided into five groups. WHO group 1 is pulmonary arterial hypertension, group 2 is PH from left-heart disease, group 3 is PH from chronic hypoxic lung disease, group 4 is PH from chronic blood clots, and group 5 is PH from unclear multifactorial mechanisms (sarcoidosis, hematologic disorders, etc.). The pathogenesis of PH (group 1

This study was supported by National Institutes of Health National Heart, Blood, and Lung Institute [Grant R01HL132574] (to S.A.G.), American Heart Association Grant-in-Aid [Grant 17GRNT33670454] (to S.A.G.), and Cancer Research UK [Grants C480/A1141 and C5759/A17098] (to A.J. and I.W.).

Some parts of the results were presented at American Heart Association Scientific Session 2019 at Philadelphia, PA.

<https://doi.org/10.1124/jpet.120.000166>.

ABBREVIATIONS: Dnmt, DNA methyltransferase; G6PD, glucose-6-phosphate dehydrogenase; Hx, hypoxia; IPA, isolation of small intrapulmonary artery; LVEDP, left ventricle end-diastolic pressure; LVSP, left ventricle end-systolic pressure; mAP, systemic mean arterial pressure; PASMC, pulmonary artery smooth muscle cell; PDD4091, *N*-[(3 β ,5 α)-17-oxoandrostan-3-yl]sulfamide; PH, pulmonary hypertension; PPP, pentose phosphate pathway; RV, right ventricle; RVEDP, RV end-diastolic pressure; RVSP, RV systolic pressure; SMC, smooth muscle cell; SU, Sugeng5416; Tet, ten-eleven translocation.

and group 2) is still unclear. PH occurs under sustained environmental stress such as inflammation, shear stress, and hypoxia. These stress stimuli contribute to the shifting of pulmonary vascular cells to hyperproliferative and apoptotic-resistant phenotypes, allowing abnormal vascular remodeling and PH development (Boucherat et al., 2017; D'Alessandro et al., 2018). Pulmonary vascular cells in patients with PH also undergo metabolic adaptation to support their high rate of proliferation or inadequate rates of mitotic fission. This metabolic shift, the Warburg phenomenon (Warburg et al., 1927), is a failure of mitochondrial respiration and activation of aerobic glycolysis.

The pentose phosphate pathway (PPP)—a branch of glycolysis and a fundamental glucose metabolism pathway—is vital for cell growth and survival. Glucose-6-phosphate dehydrogenase (G6PD) is the first rate-limiting enzyme of the PPP. G6PD and the PPP generate pentose sugar, which is required for the de novo cellular synthesis of RNA and DNA, and NADPH, a key cofactor for reductive and anabolic reactions. Recently, we found that inhibition and knockdown of G6PD in lungs of a chronic hypoxia-induced PH mouse model reduced and reversed 1) the Warburg phenomenon, 2) epigenetic modification (DNA methylation), 3) maladaptive expression of genes that support pulmonary artery remodeling, and 4) PH and left-heart dysfunction (Joshi et al., 2020). However, the role of G6PD in the pathogenesis of hypoxia + Sugen5416-induced PH is unknown. Furthermore, whether inhibition of G6PD reduces remodeling of pulmonary artery and PH in the hypoxia + Sugen5416 mouse model remains to be determined. We hypothesized that G6PD is a safe pharmacotherapeutic target to reduce PH in the hypoxia + Sugen5416 mouse model. Therefore, our objectives were to determine whether the inhibition of G6PD activity by pharmacologic manipulations would decrease differential DNA methylation and maladaptive gene expression in lungs and pulmonary vascular cells, reduce vascular remodeling, and normalize hemodynamics in models of chronic hypoxia- and hypoxia + Sugen5416-induced PH (groups 3 and 1, respectively).

Materials and Methods

Drugs and Reagents. All chemicals and reagents were purchased from Sigma, Thermo Fisher Scientific, and VWR.

Animal Models and Experimental Protocols. All animal experiments were approved by the New York Medical College Animal Care and Use Committee, and all procedures conformed to the guidelines from the NIH Guide for the Care and Use of Laboratory Animals. Male and female C57BL/6J mice (18–32 g) were purchased from the Jackson Laboratory and were randomly divided into four groups: normoxia (Nx), normoxia + Sugen5416 (Nx + SU), hypoxia (Hx), and hypoxia + Sugen5416 (Hx + SU) groups. Mice in the Nx group were placed in a normoxic (21% O₂) environment, and mice in the Hx group were placed in a normobaric hypoxic chamber (10% O₂) for 6 weeks (Joshi et al., 2020). Mice in the Nx + SU and Hx + SU groups received subcutaneous injection of SU5416 (20 mg/kg) once weekly during 3 weeks of Nx (21% O₂) or Hx (10% O₂) as previously described (Vitali et al., 2014). Mice in the drug treatment groups received daily subcutaneous injection of a novel G6PD inhibitor, N-[(3β,5α)-17-oxoandrostan-3-yl]sulfamide (PDD4091; 1.5 mg kg⁻¹ day⁻¹) (Hamilton et al., 2012), for 3 weeks. To determine whether PDD4091 reduces PH in a dose-dependent manner, mice were randomized to receive low-dose (0.15 mg kg⁻¹ day⁻¹), medium-dose (1.5 mg kg⁻¹ day⁻¹), or high-dose (15 mg kg⁻¹ day⁻¹) injections of PDD4091. Hx and Hx + SU mice are preclinical models of PH (Stenmark et al., 2009). At the end of the treatment period,

hemodynamic measurements were performed, tissue (lungs and arteries) was harvested, and blood samples were collected. Data analysis was performed in a blinded fashion.

Hemodynamic Measurements. All mice were anesthetized with inhalation of isoflurane (isoflurane, USP; 1-chloro-2,2,2-trifluoroethyl difluoromethyl ether; induced at 3% and maintained at 1.5%) and placed on a heated table. Closed-chest cardiac catheterization was performed using an MPVS Ultra Single Segment Pressure-Volume Unit (Millar Instruments) in combination with a cardiac catheter. RV systolic pressure (RVSP) and RV end-diastolic pressure (RVEDP) were measured by catheterization of the RV via the right external jugular vein using Millar Mikro-Tip catheter (model SPR-671, tip size of 1.4F; Millar Instruments). The catheter was then removed, and the jugular vein was tied off. For hemodynamic measurements from LV, the right carotid artery was dissected, and a Millar Mikro-Tip conductance catheter (model SPR-839, tip size of 1.4F; Millar Instruments) was introduced into the artery and advanced into the LV via the aortic valve. Once steady-state hemodynamics were achieved, pressure-volume loops were recorded and analyzed using LabChart 8 software (ADInstruments).

Hematocrit Measurements and Blood Chemistry Analysis. After hemodynamic measurements were completed, blood was collected from the cardiac chambers into a heparinized syringe. Heparinized blood was placed in capillary tubes, and hematocrit (%) was calculated as the length of the erythrocyte layer divided by the length of the entire blood sample. Plasma was shipped to Antech Diagnostics (NC), a GLP facility, where blood tests were performed with routinely used clinical laboratory diagnostic tools.

Assessment of Right Ventricular Hypertrophy. After the cardiac catheterization, the animals were euthanized by cervical dislocation, whole hearts were excised, and RV free wall and LV including ventricular septum (S) were separated and weighed independently. Fulton's index (RV/LV + S ratio) was calculated as an index of RV hypertrophy.

Isolation of Small Intrapulmonary Arteries and IPA Tone Measurements. Mice (25–30 g) were sacrificed by cervical dislocation, and small intrapulmonary arteries (IPA) of third order (100–150 μm in diameter) were isolated from the lung, dissected free of connective tissue, and placed in Krebs' bicarbonate buffer solution (pH 7.4) containing the following (in millimolars): 118 NaCl, 4.7 KCl, 1.5 CaCl₂ × 2H₂O, 25 NaHCO₃, 1.1 MgSO₄, 1.2 KH₂PO₄, 5.6 glucose, and 10 HEPES. Then, the vessels were mounted on a wire myograph (Danish Myo Technology A/S, Aarhus, Denmark) and bathed in Krebs' buffer solution at 37°C and an optimal passive tension of 3 mN. After 30 minutes of incubation, the arterial viability and equilibration were assessed by the stimulation of the vessels with repeated 10-minute exposures to KCl (60 mM; 60 K). For registration of vascular ring contractile activity and its following analysis, Chart 5.5.4 and LabChart Reader 8.1.9 (ADInstruments, Inc.) software were used. Vascular tension is presented as a percentage of the maximum steady-state contraction level obtained to the exposure to 60 K.

RNA-seq Analysis. After collecting lungs from Nx, Hx, and Hx + SU mice, total RNA was isolated from tissue using the Qiagen All Prep DNA/RNA/miRNA Universal kit according to manufacturer's instructions. RNA was quantified using the NanoDrop (Thermo Fisher Scientific), and quality was assessed using the Agilent Bioanalyzer 2100. RNA-seq library construction was performed using the TruSeq Stranded Total RNA Preparation kit (Illumina) with 200 ng of RNA as input according to the manufacturer's instructions. Libraries were sequenced on the HiSeq2500 with single-end reads of 100 nt at the University of Rochester Genomics Research Center. Single-end sequencing was done at a depth of 10 million reads per replicate. Quantitative analysis, including statistical analysis of differentially expressed genes, was done with Cufflinks 2.0.2 and Cuffdiff2 (<http://cufflinks.cbcb.umd.edu>). The Benjamini-Hochberg method was applied for multiple test correction (FDR < 0.05).

Reduced Representation Bisulfite Sequencing. To determine DNA methylation status in lungs of Nx, Hx, Hx + SU, and Hx + 4091

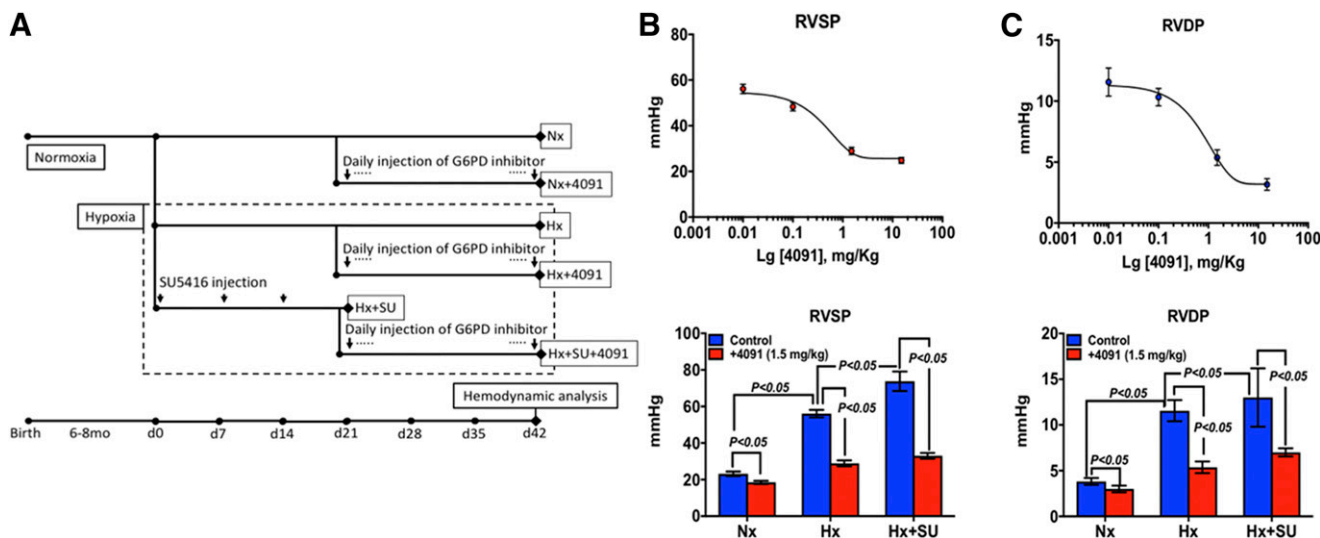


Fig. 1. Daily injection of a novel G6PD inhibitor, PDD4091, decreased pulmonary artery remodeling and right ventricle pressure and hypertrophy in mice elicited by hypoxia and hypoxia + Sugen5416. (A) A schematic showing various treatment protocols in C57BL/6J mice in normoxia and hypoxia and mice treated with Sugen5416 (20 mg kg⁻¹) once a week. (B and C) RVSP and right ventricle diastolic pressure (RVDP) were reduced dose-dependently by PDD4091 treatment of 3 weeks to hypoxic mice. PDD4091 (1.5 mg kg⁻¹ day⁻¹) for 3 weeks reduced RVSP and RVDP in mice exposed to hypoxia and hypoxia + Sugen5416. *N* = 11, normoxia; *N* = 6, normoxia + 4091; *N* = 9, hypoxia; *N* = 6, hypoxia + 4091 (0.10 mg kg⁻¹ day⁻¹); *N* = 11, hypoxia + 4091 (1.5 mg kg⁻¹ day⁻¹); *N* = 6, hypoxia + 4091 (15 mg kg⁻¹ day⁻¹); *N* = 5, hypoxia + Sugen5416 (20 mg kg⁻¹); and *N* = 5, hypoxia + Sugen5416 (20 mg kg⁻¹) + 4091 (1.5 mg kg⁻¹ day⁻¹). Each group included male and female mice (2:1 ratio). Statistical analysis was performed using two-way ANOVA and Sidak's test for multiple comparisons.

mice, genomic DNA was isolated from lungs using the Qiagen All Prep DNA/RNA/miRNA Universal kit according to the manufacturer's instructions. DNA was quantified using the NanoDrop (Thermo Fisher Scientific) and Qubit Fluorometer (Thermo Fisher Scientific). Genomic DNA quality was assessed using the Agilent TapeStation. Reduced representation bisulfite sequencing library construction was performed with the Premium Reduced Representation Bisulfite Sequencing Kit (Diagenode) following the manufacturer's instructions. Libraries were sequenced on the HiSeq2500 with paired-end reads of 125 nt. Raw reads generated from the Illumina HiSeq2500 sequencer were de-multiplexed using bcl2fastq version 2.19.0. Quality filtering and adapter removal are performed using Trim Galore version 0.4.4_dev with the following parameters: “-paired-clip_R1 3-clip_R2 3-three_prime_clip_R1 2-three_prime_clip_R2 2” (http://www.bioinformatics.babraham.ac.uk/projects/trim_galore/). Processed and cleaned reads were then mapped to the mouse reference genome (mg38) using Bismark version 0.19.0 with the following parameters: “-bowtie2-maxins 1000.” Differential methylation analysis was performed using methylKit version 1.4.0 within an R version 3.4.1 environment. Bismark alignments were processed via methylKit in the CpG context with a minimum quality threshold of 10. Coverage was normalized after filtering for loci with a coverage of at least five reads and no more than the 99.9th percentile of coverage values. The coverage was then normalized across samples, and the methylation counts were aggregated for 500-nt windows spanning the entire genome. A unified window set across samples was derived such that only windows with coverage by at least one sample per group were retained. Differential methylation analysis between conditional groups was performed using the χ^2 test and applying a *q*-value (SLIM) threshold of 0.05 and a methylation difference threshold of 25%.

Quantitative Real-Time PCR. Real-time RT-PCR technique was used to analyze mRNA expression. Briefly, total RNA was extracted from lungs using a Qiagen miRNEasy kit (217004). The input RNA quality and concentration were measured on the Synergy HT Take3 Microplate Reader (BioTek, Winooski, VT), and cDNA was prepared using SuperScript IV VILO Master Mix (11756500; Invitrogen) for mRNA. Quantitative PCR was performed in duplicate using TaqMan Fast Advanced Master Mix (44-445-57) for mRNA using a Mx3000p Real-Time PCR System (Stratagene, Santa Clara,

CA). The primers for the QPCR were purchased from Thermo Fisher Scientific/TaqMan. Results for mRNA expression were normalized to internal control *Tuba1a*, and relative mRNA expression was determined using the $\Delta\Delta C_t$ method.

Cell Culture. Human pulmonary artery smooth muscle cells (PASMCs; Lonza) were maintained at 37°C under 5% CO₂ in smooth muscle basal media (CC-3181; Lonza) supplemented with growth factors (SMGM-2 smooth muscle singlequots kit, CC-4149; Lonza). Once cells reached approximately 70% confluence, they were subcultured using 0.05% trypsin-EDTA (25300-054; GIBCO, Thermo Fisher Scientific, Grand Island, NY) into six-well plates at about 3×10^5 cells per well.

Statistical Analysis. Statistical analysis was performed using GraphPad Prism 5 software. Values are presented as means \pm S.E. Statistical comparisons of samples were performed with two-way ANOVA followed by Sidak's post hoc test for multiple comparisons and Student's *t* test for comparing two groups. Differences with *P* < 0.05 between the groups were considered significant.

Results

G6PD Inhibition Decreased Chronic Hx- and Hx + SU-Induced PH in Mice. PH was induced by exposing C57BL/6J mice to Hx and Hx + SU (Fig. 1A). C57BL/6J mice exposed to Hx and Hx + SU had higher RVSP and RVEDP than Nx mice (Fig. 1B). In the Nx + SU group, as compared with the Nx group, RVSP (Nx + SU: 24.6 ± 0.9 vs. Nx: 23.2 ± 1.3 ; mm Hg) and RVEDP (Nx + SU: 4.0 ± 0.4 vs. Nx: 3.8 ± 0.4 ; mm Hg) were not different. In the Hx + SU group, RVSP and RVEDP were higher than those of the Hx group (Fig. 1B).

To determine whether G6PD inhibition reduces PH, we first established the maximum tolerated dose of G6PD inhibitor (PDD4091). The maximum tolerated dose in Hx mice was 15 mg kg⁻¹ day⁻¹, beyond which PDD4091 depressed LV function. More importantly, treatment with the G6PD inhibitor PDD4091 to Hx mice decreased the elevated RVSP and RVEDP in a dose-dependent manner (Fig. 1, B and C, top panel).

TABLE 1

RV contractility and hypertrophy in Nx control vs. PH groups

The statistical differences between groups was determined by two-way ANOVA followed by Sidak's post hoc test.

	Nx (<i>n</i> = 11)	Nx + 4091 (<i>n</i> = 6)	Hx (<i>n</i> = 9)	Hx + 4091 (<i>n</i> = 11)	Hx + SU (<i>n</i> = 7)	Hx + SU + 4091 (<i>n</i> = 6)
RV dP/dt max (mm Hg/s)			1664 ± 391	1343 ± 289	2706 ± 703*	1647 ± 114 [†]
RV -dP/dt min (mm Hg/s)	5266 ± 1029	5890 ± 570	4945 ± 788	4753 ± 553	4648 ± 1099	4504 ± 1302
Fulton's index, RV/LV + S	0.225 ± 0.035	0.249 ± 0.040	0.385 ± 0.080***	0.202 ± 0.032 ^{§§§}	0.388 ± 0.030***	0.291 ± 0.031 ^{†††}

P* < 0.05; *P* < 0.001; ****P* < 0.0001, comparison with Nx; §*P* < 0.05; §§*P* < 0.01; §§§*P* < 0.001, comparison with Hx; [†]*P* < 0.05; ^{††}*P* < 0.001; ^{†††}*P* < 0.0001, comparison with SuHx.

PDD4091 had a reasonably wide therapeutic window (0.01–15 mg kg⁻¹ day⁻¹) with an EC₅₀ of 0.26 ± 0.10, and 0.58 ± 0.36 mg kg⁻¹ day⁻¹ reduced both RVSP and RVEDP. Moreover, PDD4091 (1.5 mg kg⁻¹ day⁻¹) treatment to both Hx and Hx + SU mice efficaciously reduced the elevated RVSP and RVEDP (Fig. 1, B and C, bottom panel). Fulton's index was increased in Hx and Hx + SU groups as compared with Nx and Nx + SU groups. G6PD inhibitor reduced elevated Fulton's index in Hx and Hx + SU groups (Table 1). In addition, PDD4091 (1.5 mg kg⁻¹ day⁻¹) treatment to mice (*n* = 6) with preexisting Hx + SU-induced PH reduced RVSP (from Hx + SU: 74 ± 5.3 to Hx + SU + PDD4091: 41 ± 3.3 mm Hg; *P* < 0.05), RVEDP (from Hx + SU: 13 ± 3 to Hx + SU + PDD4091: 7 ± 1 mm Hg; *P* < 0.05), and Fulton's index (from Hx + SU: 0.4 ± 0.01 to Hx + SU + PDD4091: 0.3 ± 0.01; *P* < 0.05). PDD4091 (1.5 mg kg⁻¹ day⁻¹) reduced G6PD activity by 20%.

RV dP/dt had a tendency to increase in the Hx group compared with Nx and significantly increased in Hx + SU compared with Nx. PDD4091 treatment (1.5 mg kg⁻¹ day⁻¹; Table 1) normalized RV dP/dt in the Hx + SU group. LV hemodynamic and function parameters are shown in Table 2. There were no significant differences in mAP, LVSP, LVEDP, and dP/dt in the Hx and Hx + SU groups.

Next, we determined the effect of PPD4091 on hematocrit and organ (such as liver, pancreas, and kidney) function. As expected, mice exposed to Hx had higher hematocrit than Nx (Table 2). Treating Hx mice with PDD4091 (1.5 mg kg⁻¹ day⁻¹) for 3 weeks reduced the elevated hematocrit in Hx mice (Table 2). The blood chemistry analysis revealed that PDD4091 treatment normalized electrolyte levels and did not alter organ function in Hx mice (Table 3).

G6PD Inhibition Relaxed Precontracted PA, Decreased PASMCGrowth, and Reduced PA Remodeling in Hx + SU Mice. PA remodeling is the hallmark of severe PH. Hyperplastic and apoptosis-resistant PA endothelial cells and PSMCs contribute to hypertensive remodeling (Morrell et al., 2009). Previously, we and others proposed that SMCs

switch from a differentiated to a dedifferentiated phenotype in PA of hypertensive patients and animals and contribute to PA remodeling (Zhou et al., 2009; Chettimada et al., 2015; Sahoo et al., 2016). Dedifferentiated SMCs are hyperproliferative, migratory, and secretory (Frisman et al., 2018). Previous studies show that the Hx + SU mouse model of PH has more severe PA remodeling than Hx mice (Vitali et al., 2014). Therefore, we determined whether G6PD inhibition relaxes PA in ex vivo studies, stunts the growth of PSMCs exposed to Hx and SU in cell culture, and reduces remodeling of PA in Hx + SU mice. Our results demonstrated PDD4091 dose-dependently relaxed PA precontracted with KCl (Fig. 2A). Application of PDD4091 [1 μmol/l, an EC₅₀ dose (Hamilton et al., 2012)] for 48 hours to PSMCs cultured in normoxia decreased cell numbers (Fig. 2B) and in addition attenuated the cell growth evoked by Hx and Hx + SU (Fig. 2C). Treatment of Hx + SU mice with PDD4091 (1.5 mg kg⁻¹ day⁻¹) for 3 weeks abrogated the occlusive pulmonary vascular remodeling (Fig. 2D).

Gene Expression Is Altered in Lungs of Hx and Hx + SU Mice. To discover the genetic and/or epigenetic determinants of PSMC growth in the PA wall and remodeling of PA in Hx and Hx + SU, we performed RNA-seq analysis in lungs of mice exposed to Nx, Hx, and Hx + SU. Several thousand genes (total 33,141) were upregulated (15,412) or downregulated (17,729) in lungs of mice exposed to Hx and Hx + SU as compared with Nx. The results revealed that out of 159 and 97 genes upregulated (≥1.5log₂_fold; *P* < 0.05) in lungs of Hx versus Nx and Hx + SU versus Nx mice, respectively, only three genes were commonly upregulated in both groups (Fig. 3A), whereas out of 1511 and 1523 genes that were downregulated (≥1.5log₂_fold; *P* < 0.05) in lungs of Hx versus Nx and Hx + SU versus Nx mice, respectively, 1085 genes were commonly downregulated in both groups (Fig. 3A). Transcription factor binding site enrichment analysis using oPOSSUM (Kwon et al., 2012) disclosed TCF21, KLF4, and E2F1 as the most enriched TFBS in

TABLE 2

Systemic blood pressure, LV hemodynamic, and hematocrit changes in Nx control and treatment groups

The statistical differences between groups was determined by two-way ANOVA followed by Sidak's post hoc test.

	Nx (<i>n</i> = 11)	Nx + 4091 (<i>n</i> = 6)	Hx (<i>n</i> = 9)	Hx + 4091 (<i>n</i> = 11)	SuHx (<i>n</i> = 7)	SuHx + 4091 (<i>n</i> = 6)
b.wt. (g)	23 ± 3	26 ± 5	24 ± 3	23 ± 3	25 ± 3	26 ± 2
HR (bpm)	455 ± 71	508 ± 71	455 ± 36	466 ± 34	519 ± 19	408 ± 52 ^{††}
mAP (mm Hg)	87.7 ± 12.4	76.5 ± 4.0*	88.3 ± 6.7	85.4 ± 4.8	82.2 ± 15.3	85.0 ± 4.0
LVSP (mm Hg)	104.0 ± 11.2	95.5 ± 3.9	104.8 ± 5.7	96.8 ± 3.9	101.8 ± 21.2	97.9 ± 4.6
LVEDP (mm Hg)	11.2 ± 2.8	6.2 ± 3.2	15.2 ± 3.2	10.7 ± 1.9	16.5 ± 9.9	7.9 ± 2.3
dP/dt max (mm Hg/s)	5841 ± 803	6385 ± 462	5559 ± 496	5567 ± 668	6021 ± 1114	5510 ± 1302
-dP/dt min (mm Hg/s)	5266 ± 1029	5890 ± 570	4945 ± 788	4753 ± 553	4648 ± 1099	4504 ± 1302
Ht (%)	46 ± 3	44 ± 2	60 ± 3***	48 ± 6 ^{§§§}	59 ± 3***	56 ± 4

HR, heart rate; Ht, hematocrit.

P* < 0.05; *P* < 0.001; ****P* < 0.0001, comparison with Nx; §*P* < 0.05; §§*P* < 0.01; §§§*P* < 0.001, comparison with Hx; [†]*P* < 0.05; ^{††}*P* < 0.001; ^{†††}*P* < 0.0001, comparison with SuHx.

TABLE 3
Blood chemistry in mice
The statistical differences between groups were determined by two-way ANOVA followed by Sidak's post hoc test.

Blood Parameters	Nx	Hx	Hx + 4091
Blood urea nitrogen (mg/dl)	31.3 ± 3.8	31.8 ± 1.4	36.0 ± 2.0
Creatinine (mg/dl)	0.23 ± 0.03	0.20 ± 0.0	0.23 ± 0.03
Glucose (mg/dl)	115 ± 33	127 ± 18	145 ± 19
Na ⁺ (mmol/l)	162 ± 1	182 ± 2*	168 ± 3 [#]
K ⁺ (mmol/l)	4.6 ± 0.4	3.5 ± 0.1*	4.8 ± 0.4 [#]
Cl ⁻ (mmol/l)	125 ± 1	118 ± 1*	127 ± 3 [#]
Alkaline phosphatase (U/l)	49 ± 4	68 ± 8*	40 ± 4 [#]
Alanine aminotransferase (U/l)	9 ± 2	6 ± 1	5 ± 2
Aspartate aminotransferase (U/l)	75 ± 6	106 ± 28	75 ± 2
Total bilirubin (mg/dl)	0.1 ± 0.0	0.1 ± 0.0	0.1 ± 0.0
Direct bilirubin (mg/dl)	0 ± 0	0 ± 0	0 ± 0
Lactate dehydrogenase (U/l)	374 ± 78	367 ± 39	449 ± 22
Creatine kinase (U/l)	254 ± 57	268 ± 68	136 ± 21
Total protein (g/dl)	3.6 ± 0.1	3.2 ± 0.1*	3.7 ± 0.1 [#]
Albumin (g/dl)	2.1 ± 0.1	1.1 ± 0.1*	2.1 ± 0.1 [#]
Ca ²⁺ (mg/dl)	7.6 ± 0.2	6.6 ± 0.1*	7.2 ± 0.2 [#]
PHOS (mg/dl)	9.2 ± 1.7	8.3 ± 0.9	9.4 ± 1.2
Mg ⁺ (mg/dl)	2.2 ± 0.1	2.2 ± 0.1	2.3 ± 0.3
Cholesterol (mg/dl)	44 ± 8	52 ± 3	66 ± 7
Triglycerides (mg/dl)	46 ± 13	82 ± 15	64 ± 9
Amylase (U/l)	406 ± 64	300 ± 13	387 ± 34
Lipase (U/l)	87 ± 20	45 ± 6*	42 ± 7*

The statistical differences between groups was determined by two-way ANOVA followed by Sidak's post hoc test.
**P* < 0.05 vs. Nx and [#]*P* < 0.05 vs. Hx.

genes upregulated in the Hx group and HIF1A::ARNT, KLF4, and SP1 as the most enriched TFBS in genes upregulated in the Hx + SU group (Fig. 3B, top panels). HOXA5, PDX1, and PRRX2 were the most enriched TFBS in genes downregulated in the Hx and Hx + SU groups (Fig. 3B, bottom panels). Suppressor of fused (*Sufu*) homolog and *Cyp1a1* genes, respectively, upregulated >100- and >15-fold in lungs of mice exposed to Hx + SU, but not to Hx, and all genes downregulated >20-fold were common in lungs of mice exposed to Hx + SU and Hx (Fig. 3C).

G6PD Inhibition Decreased Expression of *Cyp1a1* and *Sufu* Genes in Lungs of Mice and in Human PSMCs Exposed to Hx + SU. Next, we determined whether inhibition of G6PD activity decreases expression of *Cyp1a1* and *Sufu*, which are increased in lungs of hypertensive mice (Fig. 3C) and Hx and Hx + SU mice and in human PSMCs exposed to Hx + SU. Treatment of PDD4091 (1.5 mg kg⁻¹ day⁻¹) for 3 weeks to mice and application of PDD4091 (1 μM) to human PSMCs for 48 hours rescinded the Hx + SU-induced *Cyp1a1* and *Sufu*

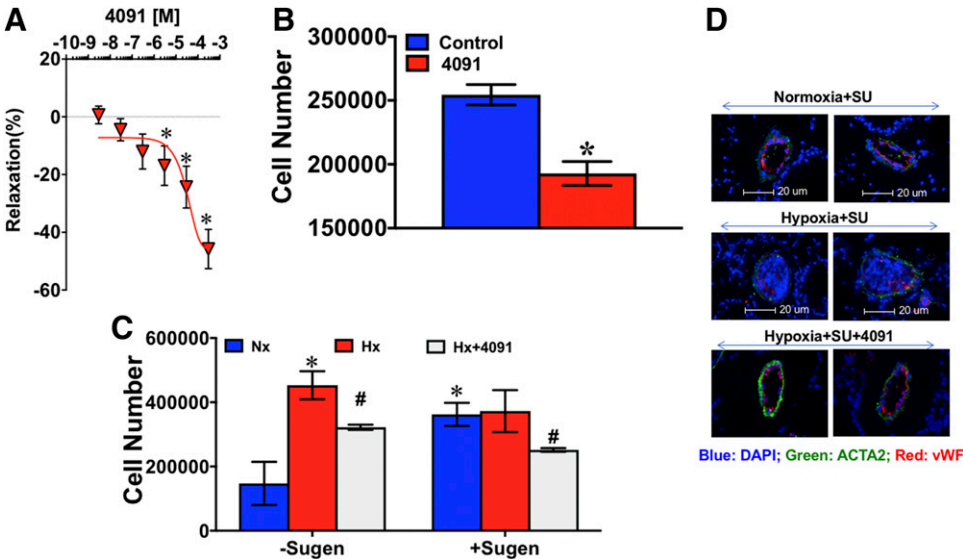


Fig. 2. G6PD inhibitor, PDD4091, relaxed precontracted PA, decreased PSMC growth, and rescinded occlusive lesion in PA. (A) Application of PDD4091 dose-dependently relaxed the pulmonary arterial rings precontracted with KCl (30 mM); *N* = 6 in each dose. (B) Application of PDD4091 (1 μmol/l) to human pulmonary artery smooth muscle cells for 48 hours decreased growth of cells cultured in 21% O₂; *N* = 6. (C) Hypoxia (3% O₂; *N* = 6) and Sugen (1 μmol/l; *N* = 6), as compared with normoxia control (21% O₂; *N* = 6), increased human pulmonary artery smooth muscle cell numbers, and application of PDD4091 (1 μmol/l; *N* = 6) to cells for 48 hours reduced their growth. (D) Immunofluorescent micrograph shows occluded pulmonary artery in lungs of mice exposed to hypoxia + SU, and occluded pulmonary arteries were not present in lungs of hypoxia + SU mice treated with PDD4091 for 3 weeks. *N* = 4 in normoxia; hypoxia + SU and hypoxia + SU + 4091 groups. **P* < 0.05 vs. 3 × 10⁻⁹ M in (A). **P* < 0.05 vs. control or Nx, and [#]*P* < 0.05 vs. hypoxia in (B and C). Statistical analysis was performed by one-way ANOVA in (A and C) and by Student's *t* test in (B).

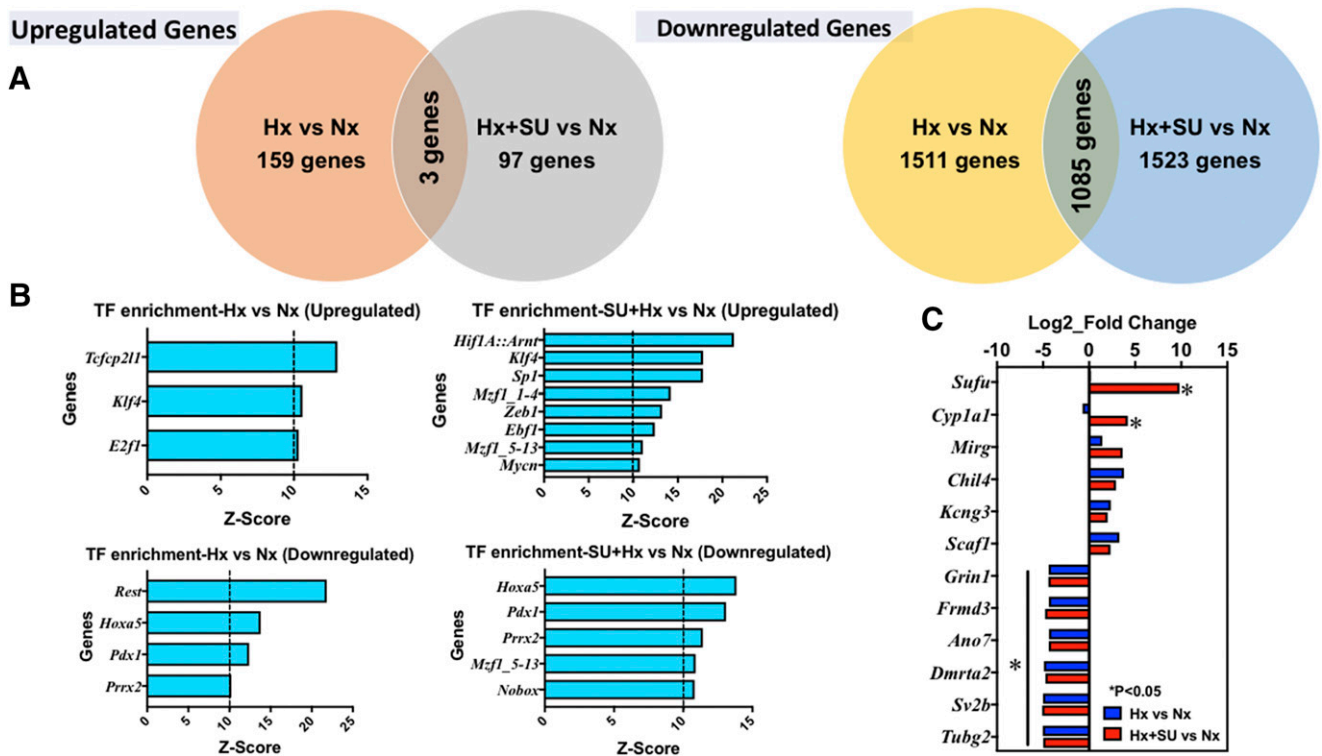


Fig. 3. Gene expression in lungs of mice exposed to hypoxia and hypoxia + Sugen5416. (A) Venn diagram of whole-genome RNA-seq analysis demonstrates that three genes are common in the significantly upregulated cohort and that 1085 genes are common in the significantly downregulated cohort in lungs of mice exposed to Hx and Hx + SU compared with normoxia control (Nx). (B) Transcription factor binding site enrichment analysis using oPPOSUM revealed that TCFCP2L1 and KLF4 in Hx vs. Nx and HIF1A:ARNT and KLF4 in Hx + SU vs. Nx are the most enriched TFBS in the upregulated genes category, and REST and HOXA5 in Hx vs. Nx and HOXA5 and PDX1 in Hx + SU vs. Nx are the most enriched TFBS in the downregulated genes category in mouse lungs. (C) RNA-seq results demonstrate *Sufu* and *Cyp1a1* genes are the most upregulated in lungs of mice exposed to Hx + SU vs. Nx but not to Hx vs. Nx, and *Tubg2* and *Sv2b* genes are the most downregulated in lungs of mice exposed to Hx + SU vs. Nx and to Hx vs. Nx. RNA-seq was performed on three lungs in each group. Male = 2 and female = 1. For statistical analysis, the Benjamini-Hochberg method was applied for multiple test correction (FDR < 0.05).

expression in lungs (Fig. 4, A and B) and in human PASMCs (Fig. 4C).

Methylation of DNA Is Decreased in Lungs of Hx and Hx + SU Mice. Epigenetic modifications are incriminated in the pathogenesis of PH (Cheng et al., 2019). Recently, we reported that downregulation of ten-eleven translocation 2 (*Tet2*) DNA demethylase in lungs of Hx Sv129J mice lacking the *Cyp2c44* gene contributes to the genesis of PH and also

demonstrated that inhibition of G6PD was ineffective in reducing PH in hypoxic *Tet2*^{-/-} mice (Joshi et al., 2020). Therefore, we assumed that downregulation of *Tet2* by Hx may augment DNA methylation in C57BL/6J mice and mediate maladaptive gene expression. Unexpectedly, we found that expression of *Tet1*, but not of *Tet2* or *Tet3*, was reduced in lungs of C57BL/6J mice exposed to Hx (Fig. 5A; Table 4). In addition, expression of *Dnmt3b*, but not of *Dnmt3a*

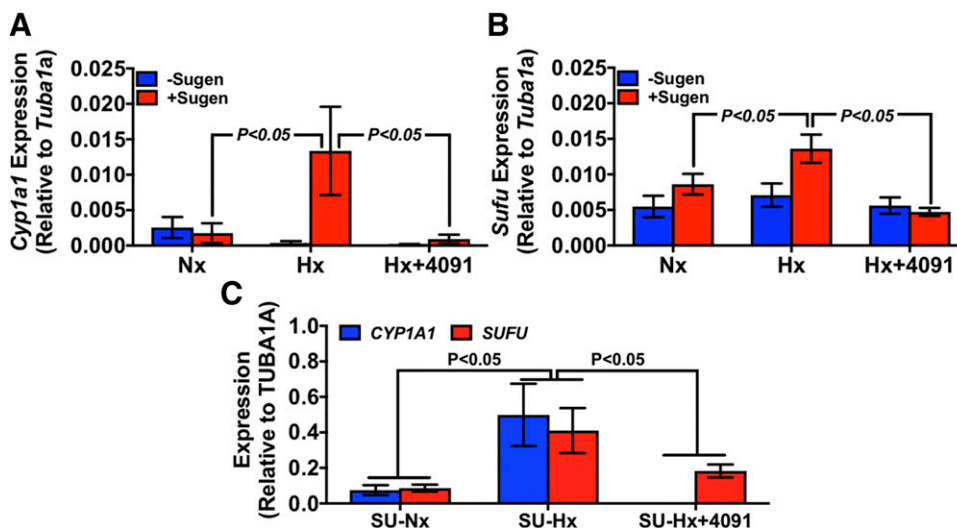


Fig. 4. Expression of *Cyp1a1* and *Sufu* genes is decreased by the G6PD inhibitor PDD4091. (A and B) Real-time PCR results confirmed RNA-seq results that *Cyp1a1* and *Sufu* are increased in lungs of mice exposed to Hx + SU but not to Hx and that PDD4091 treatment decreased *Cyp1a1* and *Sufu*. *N* = 5 (male = 3, and female = 2) were used for qPCR analysis in each group. (C) Expression of *CYP1A1* and *SUFU* increased in human pulmonary artery smooth muscle cells cultured in hypoxia (3% O₂), but not in normoxia (21% O₂), by Sugen5416 (1 μmol/l). Application of PDD4091 (1 μmol/l) to cells for 48 hours rescinded their elevated expression of *CYP1A1* and *SUFU*. *N* = 6 in each experimental condition. Statistical analysis was performed using two-way ANOVA and Sidak's test for multiple comparisons.

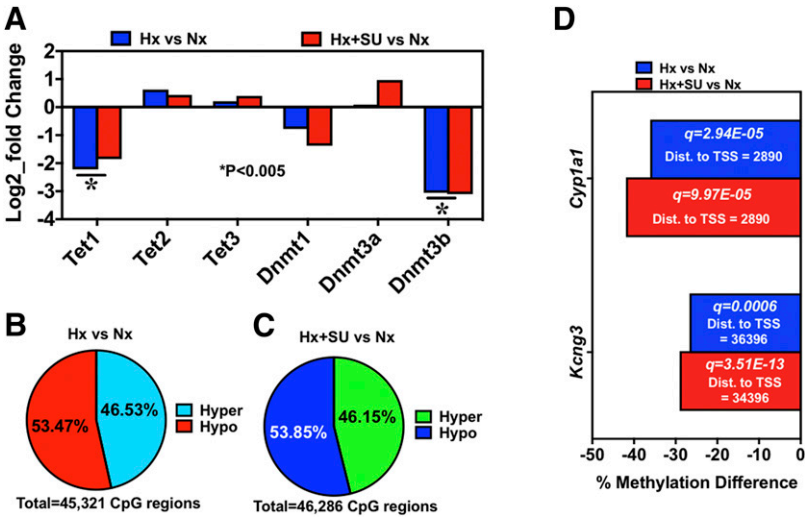


Fig. 5. DNA methylation in lungs of mice exposed to hypoxia and hypoxia + Sugen5416. (A) RNA-seq results disclosed that expression of *Tet1* and *Dnmt3b* genes is significantly decreased in lungs of mice exposed to Hx and Hx + SU as compared with Nx. *N* = 3 in each group. Methylation of the DNA in lungs of mice exposed to Nx, Hx, and Hx + SU was determined by reduced representation bisulfite sequencing method. (B and C) The pie graph demonstrates that more CpG regions are hypomethylated in lungs of Hx vs. Nx and Hx + SU vs. Nx mice. (D) *Cyp1a1* and *Kcng3* genes are hypomethylated in lungs of Hx and Hx + SU mice. The statistical differences in differential methylation between conditional groups was performed using the χ^2 test and applying a *q*-value (SLIM) threshold of 0.05 and a methylation difference threshold of 25%.

or *Dnmt1a*, was decreased (Fig. 5A; Table 4). Concomitantly, in lungs of mice exposed to Hx as compared with Nx (Fig. 5B), we found that 45,321 CpG regions were differentially methylated, out of which 46.53% regions were hypermethylated and 53.47% were hypomethylated, whereas in lungs of mice exposed to Hx + SU as compared with Nx (Fig. 5C), 46,286 CpG regions were differentially methylated, out of which 46.15% regions were hypermethylated and 53.85% were hypomethylated. Therefore, there were 0.38% more hypomethylated and less hypermethylated CpG regions in lungs of Hx + SU versus Nx than Hx versus Nx C57BL/6J mice. Furthermore, two genes, *Cyp1a1* and *Kcng3*, out of 12 upregulated genes (Fig. 3C), were hypomethylated in lungs of both Hx versus Nx and Hx + SU versus Nx C57BL/6J mice (Fig. 5D). It is noteworthy that CpG regions 2890 bp from the transcription start site of *Cyp1a1* gene were hypomethylated in both Hx versus Nx and Hx + SU versus Nx groups (Fig. 5D), and G6PD inhibition hypermethylated *Cyp1a1* and *Kcng3* genes (Table 5).

Discussion

Pharmacologic inhibition of G6PD activity with the most selective and potent inhibitor synthesized so far/to date, relaxed precontracted PA, decreased growth of PASCs evoked by Hx and SU, reduced expression of *Cyp1a1* and *Sufu*, and rescinded occlusion of PA in lungs of mice exposed to Hx + SU. Furthermore, the results of this study provided evidence that downregulation of the epigenetic modifiers *Tet1* and *Dnmt3b* and hypomethylation of DNA altered gene expression in lungs of Hx and Hx + SU mice. Since a selective inhibitor of G6PD activity decreased occlusive remodeling of PA and alleviated RVSP/heart dysfunction evoked by Hx and Hx + SU in mice, without causing organ toxicity in Hx mice, we propose that G6PD might be a safe pharmacotherapeutic target to reduce precapillary PH.

Hx and Hx + SU mouse models are routinely used to study the pathology of PH (Stenmark et al., 2009). We observed in this study that mice exposed to Hx for 6 weeks and to Hx + SU for 3 weeks developed PH, which was more severe in the Hx + SU group than in the Hx group. In chronically Hx (3 weeks) mice, vasoconstriction and muscularization of small arteries,

but not obliterative remodeling of PA, contribute to increased pulmonary arterial pressure and RV pressure overload (Stenmark et al., 2009). The more severe PH in Hx + SU mice is attributed to the formation of angio-obliterative lesions in addition to vasoconstriction and muscularization (Vitali et al., 2014). Along with vascular pathology, RV pressure and contractility increased in the Hx and Hx + SU groups. Systemic blood pressure (mAP) and LV hemodynamic (LVSP, LVEDP, and dp/dt) was not significantly different in the Hx and Hx + SU groups compared with their control groups. Thus, our results indicate that inhibition of G6PD activity reduces both remodeling of PA and elevated RV pressure overload and hypertrophy in two different mouse models of PH.

The above observations raise the question of whether the underlying genetic/epigenetic determinants of PH in mice exposed to Hx and Hx + SU are the same or different. To seek answers, we performed RNA-seq analysis in lungs, which revealed that >1000 downregulated genes and only three upregulated genes, driven by different transcription factors, were common between the two models. Most strikingly, expression of *Sufu* and *Cyp1a1* genes increased >15-fold in lungs of mice exposed to Hx + SU but not to Hx. Furthermore, exposure to SU increased expression of both *SUFU* and *CYP1A1* genes in Hx but not in Nx human PASCs. Although these results are consistent with a recent study that indicates the HIF::ART-driven *Cyp1a1* gene is upregulated in lungs of rats exposed to SU/Hx/Nx and in human PASCs by SU (Dean et al., 2018), an increase of *Sufu* in lungs of PH mice and human PASCs has not been reported. CYP1A1 is an

TABLE 4
Expression of *Dnmt* and *Tet* genes in mouse lungs
For statistical analysis, the Benjamini-Hochberg method was applied for multiple test correction (FDR < 0.05).

Genes	Hx vs. Nx		Hx + SU5149 vs. Nx	
	Log ₂ fold	P Value	Log ₂ fold	P Value
<i>Dnmt1</i>	−0.775	0.1700	−1.377	0.0158
<i>Dnmt3a</i>	0.086	0.8400	0.969	0.0200
<i>Dnmt3b</i>	−3.056	0.0028	−3.101	0.0032
<i>Tet1</i>	−2.219	0.0195	−1.852	0.0472
<i>Tet2</i>	0.628	0.2479	0.440	0.4165
<i>Tet3</i>	0.212	0.4949	0.402	0.1886

TABLE 5

Methylation status of *Cyp1a1* and *Kcng3* genes in mouse lungsThe statistical differences in differential methylation between conditional groups was performed using the χ^2 test and applying a *q*-value (SLIM) threshold of 0.05 and a methylation difference threshold of 25 percent.

Condition	Gene Name	Strand	Distance from TSS	Differential Methylation	<i>q</i> -Value (SLIM)
				%	
Hx vs. Nx	ENSMUST00000034865.4_Cyp1a1	+	2890	−36.1	1.42E−05
		+	3890	−25.1	0.00366025
		+	4390	−31.4	2.25E−13
Hx + SU vs. Nx	ENSMUST00000034865.4_Cyp1a1	+	2890	−41.9	3.63E−07
Hx + 4091 vs. Hx	ENSMUST00000034865.4_Cyp1a1	+	2890	36.1	7.35E−06
		+	3890	86.4	5.33E−31
		+	4390	55.0	4.27E−26
Hx vs. Nx	ENSMUST00000051482.1_Kcng3	−	36,396	−26.7	0.00044669
Hx + SU vs. Nx	ENSMUST00000051482.1_Kcng3	−	34,396	−29.1	3.44E−14
Hx + 4091 vs. Hx	ENSMUST00000051482.1_Kcng3	−	36,396	26.7	0.00245735
		−	34,396	−51.7	5.03E−26

estrogen-metabolizing enzyme that produces mitogenic metabolites of estrogen in human PSMCs (Dean et al., 2018), and *SUFU* is a negative regulator of hedgehog signaling, which controls cell proliferation during development in invertebrates and vertebrates (Briscoe and Thérond, 2013) Briscoe and Thérond, 2013; Liu, 2019). Increased CYP1A1 contributes to the pathogenesis of PH in SU/Hx/Nx rats (Dean et al., 2018). Our results suggest that increased CYP1A1 and *SUFU* signaling may have a potential role in the genesis of occlusive lesion formation in Hx + SU mice. Since transcription of *CYP1A1* was abolished and that of *SUFU* was partially decreased in mouse lungs and in human PSMCs by G6PD inhibition, transcription of *CYP1A1* and *SUFU* genes in lungs and PSMCs exposed to Hx + SU is potentially controlled by G6PD. Therefore, we propose that inhibition of G6PD activity could be useful in reversing the elevated expression of the pathogenic *CYP1A1* and *SUFU* genes in PH.

We and others have recently proposed that DNA methylation and other epigenetic modifications potentially promote maladaptive gene expression, a determinant of inflammatory and hyperproliferative cell phenotype, in remodeled PA (Hu et al., 2019; Joshi et al., 2020; Potus et al., 2020). Furthermore, we recently showed that expression of *Tet2*, a DNA demethylase considered as a master regulator of differentiated fate of SMC phenotype (Liu et al., 2013), was downregulated in lungs of Sv129J mice with a *Cyp2c44* gene knockout (Joshi et al., 2020). Therefore, we assumed that a loss of TET2 modifies DNA methylation and initiates maladaptive gene expression in lungs of mice exposed to Hx and Hx + SU. Unexpectedly, expression of *Tet1*, but not of *Tet2*, and *Dnmt3b* was downregulated in lungs of C57BL/6J mice exposed to Hx and Hx + SU. We propose that genetic variations and differences in gene regulation observed between Sv129J and C57BL/6J mice (Hashimoto et al., 2020) may be a cause of *Tet1* and *Dnmt3b* downregulation, but not of other isoforms of DNA demethylases and methyltransferases, in response to stress observed in C57BL/6J mice. TET proteins are involved in the regulation of hematopoietic stem cell homeostasis and hematologic malignancies and diseases (Nakajima and Kunimoto, 2014). Although loss of a single TET protein is not sufficient to promote malignancies (An et al., 2015), TET1 and TET2 have been shown to, respectively, repress and promote osteogenesis and adipogenesis (Cakouros et al., 2019). Furthermore, inhibition of TET1 blocks expression of large-conductance Ca^{2+} -activated K^{+} channel $\beta 1$ subunit in uterine arteries of pregnant rats (Hu et al., 2017). Expression of this channel is

a marker of differentiated SMCs. Therefore, we propose that downregulation of *Tet1* could imply that 1) SMCs are dedifferentiated and 2) decreased Ca^{2+} -activated K^{+} channels contribute to constrict PAs and increase pressure in lungs of Hx and Hx + SU mice.

Whereas inhibition of G6PD evoked hypomethylation and increased transcription of the many genes, expression of the *Cyp1a1* gene, which promotes PSMC proliferation (Dean et al., 2018), was repressed through hypermethylation of the DNA in lungs of Hx and Hx + SU mice. Therefore, these results suggest that DNA methylation modulated by G6PD is functionally important in gene regulation and substantiate our previous finding that G6PD is a regulator of DNA methyltransferases and demethylase, which plays a crucial role in remodeling of PA (Joshi et al., 2020). In contrast, transcription of *Sufu* in mouse lungs evoked by Hx + SU was not regulated by the methylation of DNA. These results suggest G6PD inhibition activated other mechanisms of gene expression in addition to differential methylation of the DNA and that these mechanisms worked synergistically to regulate gene expression in lungs of Hx and Hx + SU mice.

In addition to arresting maladaptive gene expression in vascular cells of the PA wall and reducing cell growth in occlusive pulmonary arterial disease, PDD4091—a novel and selective inhibitor of G6PD activity (Hamilton et al., 2012)—dose-dependently relaxed precontracted PAs. We have previously shown that inhibition of G6PD activity with nonspecific inhibitors, such as 17-ketosteroids [dehydroepiandrosterone (DHEA) and epiandrosterone, a DHEA metabolite], and siRNA-mediated knockdown of *G6pd* elicit relaxation of precontracted pulmonary artery (Gupte et al., 2002) and reduce RV pressures in hypertensive rats (Chettimada et al., 2012, 2015). Therefore, these studies and our current findings collectively suggest that G6PD inhibition reduces the elevated RV pressures and PH in Hx and Hx + SU mice by dilating PAs and reducing PA remodeling.

In conclusion, our results collectively demonstrate that G6PD activity is an important contributor to differential DNA methylation, maladaptive gene expression, and remodeling of PA in Hx and Hx + SU mice. The inhibition of G6PD activity by pharmacologic manipulations abrogated pulmonary vascular remodeling and improved the hemodynamics in mouse models of PH. Therefore, G6PD inhibitor *N*-[(3 β ,5 α)-17-oxoandrostan-3-yl]sulfamide might be employed in the future as a pharmacotherapeutic agent to treat different forms of PH.

Authorship Contributions

Participated in research design: Kitagawa, McMurtry, Gupte.

Conducted experiments: Kitagawa, Jacob.

Contributed new reagents or analytic tools: Jordan, Waddell.

Performed data analysis: Kitagawa, Jacob, Gupte.

Wrote or contributed to the writing of the manuscript: Kitagawa, Jacob, McMurtry, Gupte.

References

- An J, González-Avalos E, Chawla A, Jeong M, López-Moyado IF, Li W, Goodell MA, Chavez L, Ko M, and Rao A (2015) Acute loss of TET function results in aggressive myeloid cancer in mice. *Nat Commun* **6**:10071.
- Boucherat O, Vitry G, Trinh I, Paulin R, Provencher S, and Bonnet S (2017) The cancer theory of pulmonary arterial hypertension. *Pulm Circ* **7**:285–299.
- Briscoe J and Théron PP (2013) The mechanisms of Hedgehog signalling and its roles in development and disease. *Nat Rev Mol Cell Biol* **14**:416–429.
- Cakouros D, Hemming S, Gronthos K, Liu R, Zannettino A, Shi S, and Gronthos S (2019) Specific functions of TET1 and TET2 in regulating mesenchymal cell lineage determination. *Epigenetics Chromatin* **12**:3.
- Cheng X, Wang Y, and Du L (2019) Epigenetic modulation in the initiation and progression of pulmonary hypertension. *Hypertension* **74**:733–739.
- Chettimada S, Gupte R, Rawat D, Gebb SA, McMurtry IF, and Gupte SA (2015) Hypoxia-induced glucose-6-phosphate dehydrogenase overexpression and -activation in pulmonary artery smooth muscle cells: implication in pulmonary hypertension. *Am J Physiol Lung Cell Mol Physiol* **308**:L287–L300.
- Chettimada S, Rawat DK, Dey N, Kobelja R, Simms Z, Wolin MS, Lincoln TM, and Gupte SA (2012) Glc-6-PD and PKG contribute to hypoxia-induced decrease in smooth muscle cell contractile phenotype proteins in pulmonary artery. *Am J Physiol Lung Cell Mol Physiol* **303**:L64–L74.
- D'Alessandro A, El Kasmi KC, Plecité-Hlavatá L, Jezek P, Li M, Zhang H, Gupte SA, and Stenmark KR (2018) Hallmarks of pulmonary hypertension: mesenchymal and inflammatory cell metabolic reprogramming. *Antioxid Redox Signal* **28**:230–250.
- Dean A, Gregor T, Docherty CK, Harvey KY, Nilsen M, Morrell NW, and MacLean MR (2018) Role of the aryl hydrocarbon receptor in sugen 5416-induced experimental pulmonary hypertension. *Am J Respir Cell Mol Biol* **58**:320–330.
- Farber HW and Loscalzo J (2004) Pulmonary arterial hypertension. *N Engl J Med* **351**:1655–1665.
- Frismantien A, Philippova M, Erne P, and Resink TJ (2018) Smooth muscle cell-driven vascular diseases and molecular mechanisms of VSMC plasticity. *Cell Signal* **52**:48–64.
- Gupte SA, Li KX, Okada T, Sato K, and Oka M (2002) Inhibitors of pentose phosphate pathway cause vasodilation: involvement of voltage-gated potassium channels. *J Pharmacol Exp Ther* **301**:299–305.
- Hamilton NM, Dawson M, Fairweather EE, Hamilton NS, Hitchin JR, James DI, Jones SD, Jordan AM, Lyons AJ, Small HF, et al. (2012) Novel steroid inhibitors of glucose 6-phosphate dehydrogenase. *J Med Chem* **55**:4431–4445.
- Hashimoto R, Lanier GM, Dhagia V, Joshi SR, Jordan A, Waddell I, Tudor R, Stenmark KR, Wolin MS, McMurtry IF, et al. (2020) Pluripotent hematopoietic stem cells augment α -adrenergic receptor-mediated contraction of pulmonary artery and contribute to the pathogenesis of pulmonary hypertension. *Am J Physiol Lung Cell Mol Physiol* **318**:L386–L401.
- Hu CJ, Zhang H, Laux A, Pullamsetti SS, and Stenmark KR (2019) Mechanisms contributing to persistently activated cell phenotypes in pulmonary hypertension. *J Physiol* **597**:1103–1119.
- Hu XQ, Dasgupta C, Chen M, Xiao D, Huang X, Han L, Yang S, Xu Z, and Zhang L (2017) Pregnancy reprograms large-conductance Ca^{2+} -activated K^{+} channel in uterine arteries: roles of ten-eleven translocation methylcytosine dioxygenase 1-mediated active demethylation. *Hypertension* **69**:1181–1191.
- Joshi SR, Kitagawa A, Jacob C, Hashimoto R, Dhagia V, Ramesh A, Zheng C, Zhang H, Jordan A, Waddell I, et al. (2020) Hypoxic activation of glucose-6-phosphate dehydrogenase controls the expression of genes involved in the pathogenesis of pulmonary hypertension through the regulation of DNA methylation. *Am J Physiol Lung Cell Mol Physiol* **318**:L773–L786.
- Kwon AT, Arenillas DJ, Worsley Hunt R, and Wasserman WW (2012) oPOSSUM-3: advanced analysis of regulatory motif over-representation across genes or ChIP-Seq datasets. *G3 (Bethesda)* **2**:987–1002.
- Lajoie AC, Lauzière G, Lega JC, Lacasse Y, Martin S, Simard S, Bonnet S, and Provencher S (2016) Combination therapy versus monotherapy for pulmonary arterial hypertension: a meta-analysis. *Lancet Respir Med* **4**:291–305.
- Liu A (2019) Proteostasis in the Hedgehog signaling pathway. *Semin Cell Dev Biol* **93**:153–163.
- Liu R, Jin Y, Tang WH, Qin L, Zhang X, Tellides G, Hwa J, Yu J, and Martin KA (2013) Ten-eleven translocation-2 (TET2) is a master regulator of smooth muscle cell plasticity. *Circulation* **128**:2047–2057.
- Morrell NW, Adnot S, Archer SL, Dupuis J, Jones PL, MacLean MR, McMurtry IF, Stenmark KR, Thistlethwaite PA, Weissmann N, et al. (2009) Cellular and molecular basis of pulmonary arterial hypertension. *J Am Coll Cardiol* **54**(1 Suppl): S20–S31.
- Nakajima H and Kunimoto H (2014) TET2 as an epigenetic master regulator for normal and malignant hematopoiesis. *Cancer Sci* **105**:1093–1099.
- Potus F, Pauculo MW, Cook EK, Zhu N, Hsieh A, Welch CL, Shen Y, Tian L, Lima P, Mewburn J, et al. (2020) Novel mutations and decreased expression of the epigenetic regulator TET2 in pulmonary arterial hypertension. *Circulation* **141**: 1986–2000.
- Runo JR and Loyd JE (2003) Primary pulmonary hypertension. *Lancet* **361**: 1533–1544.
- Sahoo S, Meijles DN, Al Ghouleh I, Tandon M, Cifuentes-Pagano E, Sembrat J, Rojas M, Goncharova E, and Pagano PJ (2016) MEF2C-MYOC and Leiomodin1 suppression by miRNA-214 promotes smooth muscle cell phenotype switching in pulmonary arterial hypertension. *PLoS One* **11**:e0153780.
- Stenmark KR, Meyrick B, Galie N, Mooi WJ, and McMurtry IF (2009) Animal models of pulmonary arterial hypertension: the hope for etiological discovery and pharmacological cure. *Am J Physiol Lung Cell Mol Physiol* **297**:L1013–L1032.
- Vitali SH, Hansmann G, Rose C, Fernandez-Gonzalez A, Scheid A, Mitsialis SA, and Kourembanas S (2014) The Sugan 5416/hypoxia mouse model of pulmonary hypertension revisited: long-term follow-up. *Pulm Circ* **4**:619–629.
- Warburg O, Wind F, and Negelein E (1927) The metabolism of tumors in the body. *J Gen Physiol* **8**:519–530.
- Zhou W, Negash S, Liu J, and Raj JU (2009) Modulation of pulmonary vascular smooth muscle cell phenotype in hypoxia: role of cGMP-dependent protein kinase and myocardin. *Am J Physiol Lung Cell Mol Physiol* **296**:L780–L789.

Address correspondence to: Dr. Sachin A. Gupte, New York Medical College, BSB 546, 15 Dana Road, Valhalla, NY 10595. E-mail: sachin_gupte@yahoo.com or sgupte@nysmc.edu